Magnetic properties and giant magnetoresistance in melt-spun $Co_{15}Cu_{85}$ alloys

1995 J. Phys.: Condens. Matter 7 4081

(http://iopscience.iop.org/0953-8984/7/21/008)

J. Phys.: Condens. Matter 7 (1995) 4081–4093. Printed in the UK

Magnetic properties and giant magnetoresistance in melt-spun $Co_{15}Cu_{85}$ alloys

R H Yu†, X X Zhang†, J Tejada†, M Knobel‡, P Tiberto§ and P Allia§

† Department de Fisica Fonamental, Facultat de Fisica, Universitat de Barcelona, 08028 Barcelona, Spain

‡ Instituto de Física Gleb Wataghin, Universidade Estadual de Campinas, CP 6165, Campinas 13083-970 SP, Brazil

§ Dipartimento di Fisica, Politecnico di Torino, Torino, Italy

Received 7 December 1994, in final form 21 February 1995

Abstract. The structure, magnetic properties and giant magnetoresistance (GMR) of a metallic granular $Co_{15}Cu_{85}$ alloy have been investigated using an x-ray diffractometer and a SQUID magnetometer. The granular samples were fabricated by melt spinning and subsequently thermal annealing. Structural characterization confirmed that the samples consist of ultrafine Co magnetic particles embedded in the non-magnetic Cu matrix. Above the blocking temperature T_B, the magnetic behaviour of Co particles can be understood on the basis of paramagnetic theory. The largest change in magnetoresistance of 43.0% was observed for the as-quenched ribbon annealed at 450 °C. It was confirmed that the GMR is closely correlated with the Co particle size and density, which can be optimized by controlling the annealing conditions.

1. Introduction

The discovery of giant magnetoresistance (GMR) in ferromagnetic granular materials has stimulated considerable interest in spin-dependent magnetotransport properties and related phenomena [1, 2]. The substantial change in magnetoresistance (MR) in such a magnetic structure has enhanced the fundamental understanding of the physical origin of GMR, as well as offering potential application in magnetoresistive devices. Now, it is widely accepted that the GMR is closely correlated with the reorientation of the magnetic moments of particles embedded in a non-magnetic matrix and can be interpreted on the basis of electron spin-dependent scattering [3, 4]. In a granular system, the fundamental assumption underlying the GMR is that the current is carried in two independent conduction channels corresponding to the spin-down and spin-up electrons. The magnetic field dependence of the resistivity is attributed to spin-dependent scattering occurring within the magnetic particles and at the interfaces of magnetic and non-magnetic entities [5, 6]. The key parameters dominating the GMR are the mean free paths, the ratios of spin-dependent to spin-independent potentials, and the surface-to-volume ratio of the magnetic clusters [5, 6].

The GMR has been discovered in various granular systems including Cu–Co [1, 2], Cu–Fe [2], Co–Ag [7, 8] and Fe–Ni–Ag [9, 10]. The heterogeneous alloys composed of immiscible elements were fabricated by a variety of non-equilibrium techniques such as evaporation [11], sputtering [12], mechanical alloying [13, 14] and subsequent thermal annealing of the supersaturated metastable phase. Very recently, there has been growing interest in preparing metastable homogeneous Co–Cu alloys by melt spinning and studying the magnetic and

0953-8984/95/214081+13$19.50

transport properties of this system [15–18]. The granules have been produced by subsequent annealing of the as-quenched ribbons at elevated temperatures.

In this paper, we report the structural, magnetic and transport properties of melt-spun $Co_{15}Cu_{85}$ alloys. A GMR as large as 43.0% has been observed at 10 K in a magnetic field of up to 30 kOe for as-quenched ribbon annealed at 450 °C for 30 min. The GMR is shown to be strongly dependent on the Co magnetic particle sizes.

2. Experiment

A rapidly quenched $Cu_{85}Co_{15}$ alloy was prepared by planar flow casting in a controlled atmosphere on a Cu–Zr drum. The samples were cut from the ribbons 5.0×10^{-3} m in width and 6.0×10^{-5} m in thickness and subsequently subjected to furnace annealing at different temperatures in the range 350–600 °C for 30 min in a vacuum of 1.0×10^{-5} mTorr, in order to control the size and distribution of the ferromagnetic Co-rich clusters. After annealing, the samples were cooled in vacuum to room temperature in about 5 min. The oxide layer of the samples was removed using diluted acid solution. Characterization of the samples was carried out on an x-ray diffractometer with Cu $K\alpha_1$ and Cu $K\alpha_2$ radiation. The magnetic properties were obtained using a SQUID magnetometer in the temperature range 4.2–300 K. The electrical resistivity $R(H, T)$ was measured using a DC four-terminal geometry in a magnetic field of up to 50 kOe and at a temperature from 10 to 300 K. The magnetic field was applied parallel to the current and to the ribbon surface.

3. Results and discussion

3.1. Microstructure evolution and x-ray analysis

Figure 1 shows x-ray diffraction patterns for the $Co_{15}Cu_{85}$ samples in as-quenched and annealed states. The as-quenched sample is a single FCC phase, with a lattice parameter of 0.3605 nm which is less than that of bulk Cu, 0.3615 nm, but larger than the lattice constant of bulk Co, 0.3545 nm. The as-quenched sample with a lattice spacing intermediate between those of bulk Cu and bulk Co is likely to be due to the substitutional effect of Co atoms in the Cu matrix. As the annealing temperature is increased, the overall x-ray diffraction patterns do not change very much until $T_A \approx 550$ °C, where a (111) peak begins to develop distinct shoulders. Eventually, a well resolved peak indicated by an asterisk (*) is observed, corresponding to FCC Co particles. The lattice constant calculated for the Co particles in the sample annealed at $T_A = 600$ °C is 0.3555 nm, which is larger than the lattice constant of bulk Co. This result indicates that the phase precipitated from a homogeneous Cu–Co matrix is not pure Co clusters but Co-rich particles.

The stable structure of Co at room temperature is HCP; we found that the Co particles maintain an FCC structure to room temperature even when the sample was annealed at a temperature of up to 900 °C. This phenomenon could be interpreted in terms of the annealing temperature. Thermal analyses (DSC) of phase separation in metastable Co–Cu alloys have confirmed that the Co clusters usually start to precipitate at a temperature of 300 °C [14, 19]. As the as-quenched sample is annealed at temperatures above 425 °C, where the FCC phase becomes stable for bulk Co [20], there it is no doubt that the Co particles will be precipitated in FCC form. The Co particles are highly coherent with the Cu matrix, which may hinder the transformation of FCC Co to HCP Co as the temperature is decreased in order to maintain the minimum of surface energy. For the as-quenched ribbon annealed at temperatures below

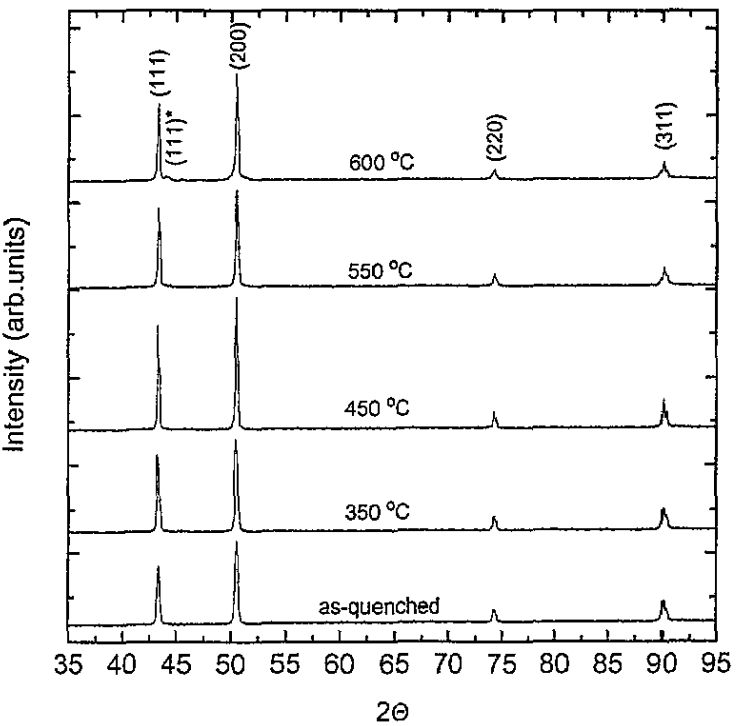

Figure 1. X-ray spectra for $Co_{15}Cu_{85}$ samples as-quenched and annealed at different temperatures. The asterisk (*) denotes the diffraction line from FCC Co clusters.

425 °C, where the HCP phase becomes stable for bulk Co, the classical nucleation theory [21] (or coherent spinodal decomposition assumption [22]), indicates that the two phases, namely the matrix and precipitates, should have the same crystal structure but different compositions. Thus the Co particles will be nucleated in the same FCC structure as the Cu matrix, and the FCC Co particles will not undergo a FCC-to-HCP transition as the samples are cooled after annealing at these temperatures. Additionally, we found that the samples are highly (200) textured in comparison with the standard bulk Cu x-ray diffraction pattern. The textured structure is not eliminated even for the sample annealed at $T_A = 900$ °C.

3.2. The magnetic properties and the size of Co particles

The 295 K magnetization curves for various samples are shown in figure 2. For the sample annealed at temperatures above 600 °C, the magnetization was found to be easily saturated using fields of just a few kilo oersteds. For the samples in the as-quenched state or annealed at a temperature below 550 °C, the magnetization does not saturate even in fields up to 30 kOe. In comparison with as-quenched ribbon, the sample annealed at $T_A = 350$ °C has a lower M_S (see figure 2). This phenomenon has been observed many times by different groups, but its physical origin is not clear at present. As the annealing temperature is increased, successive nucleation and growth of magnetic Co particles will increase the volume fraction of the Co magnetic particles and the saturation magnetization. The largest saturation magnetization of 147.38 emu g_{Co}^{-1} was observed for the sample annealed at a temperature of 550 °C. This value does not reach the M_s-values of 175 emu g^{-1} [23] and 155.2 emu g^{-1} [24] for bulk FCC Co at 5 K and 412 K, respectively, which may arise because

the Co particles contain some Cu atoms and because some Co atoms are dissolved in the Cu matrix. Very small Co particles may lose their magnetic moments owing to electron hybridizations [6]. A decrease in M_s occurs for the sample annealed at a temperature of 600 °C. This was interpreted as the increased diffusion of Co atoms back to the Cu matrix at this high temperature as assumed by Childress and Chien [25].

The particle size and distribution are important parameters of an assembly of ultrafine ferromagnetic particles. In addition to microstructural characterizations, they can be determined by analysing the magnetization curve in the superparamagnetic state. If μ_a is the moment of a Co atom and the cluster has m atoms, the total Co cluster moment will be $m\mu_a$. In reality, the magnetic cluster moment will be affected by the geometry of the clusters and also by the demagnetization effect. For a small magnetic anisotropy, the Co cluster moment will exhibit a Boltzmann distribution of the orientation with respect to the magnetic field H at thermal equilibrium. The magnetization M of a non-interacting superparamagnetic system with uniform particle size due to a classical elemental moment μ is described by a Langevin function [26, 27] $L(\alpha) = \coth\alpha - 1/\alpha$:

$$M = \mu N L\left(\frac{\mu H}{k_B T}\right) = \mu N\left[\coth\left(\frac{\mu H}{k_B T}\right) - \frac{k_B T}{\mu H}\right] \tag{1}$$

where k_B is Boltzmann's constant, N is the number of elemental moments, $\mu = M_s V$ is the magnetic moment of a single particle with volume V, and H is the external magnetic field. Using the data only for a temperature of 295 K, a least-squares fit to the magnetization data, i.e. the magnetic moment μ, can be calculated. Again, using the 5 and 412 K values of saturation magnetization for pure FCC Co, 175 emu g^{-1} (1.545×10^3 emu cm^{-3}) [23] and 155.2 emu g^{-1} (1.371×10^3 emu cm^{-3}) [24], respectively, we fitted the experimental data to equation (1); the Co particle size can be estimated. However, unsatisfactory fitting results are shown in figure 2(a). In real granular systems, there is a distribution of particle sizes, and consequently of μ. Without knowing the exact distribution of Co particle sizes, the magnetization should roughly be described by

$$M = \sum_n \mu_n N_n L\left(\frac{\mu_n H}{k_B T}\right) = \mu_1 N_1 L\left(\frac{\mu_1 H}{k_B T}\right) + \mu_2 N_2 L\left(\frac{\mu_2 H}{k_B T}\right) + \cdots + \mu_n N_n L\left(\frac{\mu_n H}{k_B T}\right) \tag{2}$$

where n represents the Co particles with the same size. Fitting the 295 K experimental $M(H)$ data to equation (2) (here we selected $n = 20$), the average Co particle sizes were determined as shown in figure 3 and table 1. The theoretical results are in good agreement with the experimental data (see figure 2(b)). It should be noted that we use M_s for pure FCC Co in the calculation; in reality, the calculated Co particle sizes should be smaller than the real particle size owing to the lower saturation magnetization for the Co–Cu samples as demonstrated above. By analysing the data obtained for the Co magnetic particles, we have confirmed that the Co particle size distribution follows a log-normal form as discussed in [28, 29]. It should be noted that the magnetization is easy to saturate for the sample annealed at 600 °C. In this case, the sample shows a complicated behaviour which may be re-entrant magnetic behaviour [23]. Here, we present the fitting result of this sample just for comparison.

Figure 4 shows the magnetic moment for the samples in both field-cooled (FC) and zero-field-cooled (ZFC) conditions, measured as a function of temperature in a small field of 50 Oe. The peaks of the ZFC curves were observed for all the samples. For $T > T_g$ the

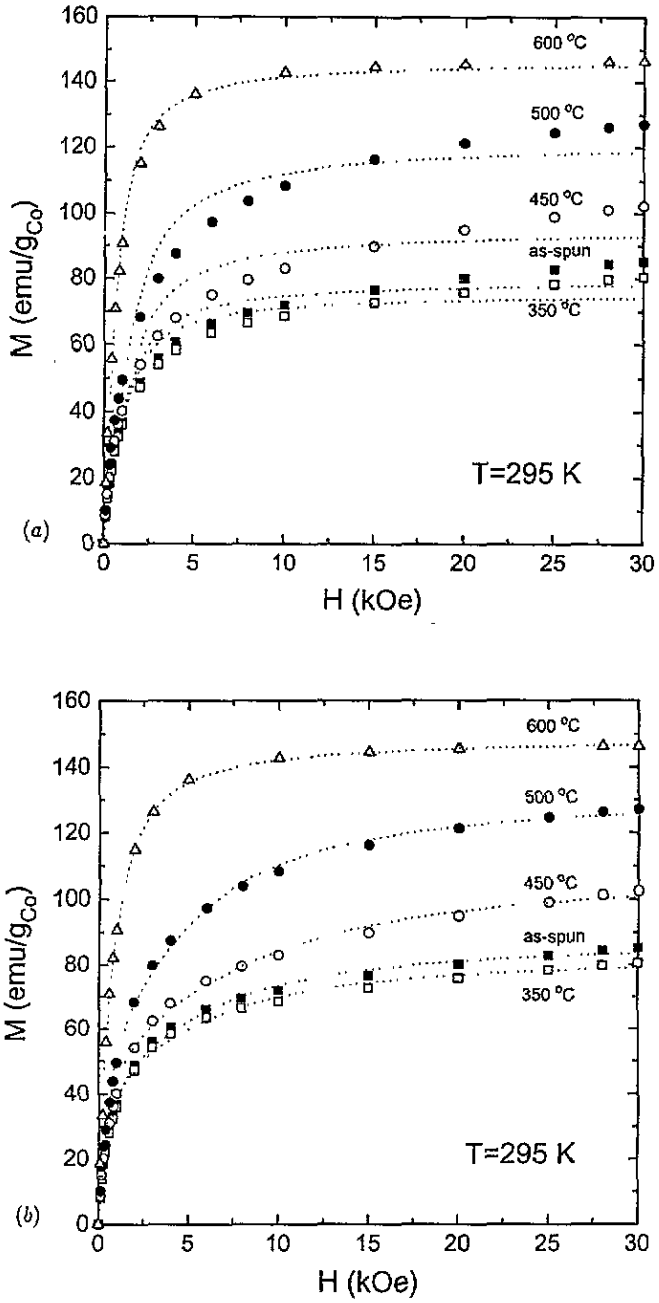

Figure 2. Room-temperature magnetization curves of $Co_{15}Cu_{85}$ ribbons in the as-quenched and annealed states. (a) on fitting with a single Co particle size and (b) on fitting with different Co particle sizes: △, ●, ○, ■, □, experimental results; – – –, theoretical values.

particles show superparamagnetic behaviour, where T_g corresponds to the maximum in the temperature dependence of the ZFC magnetization. The ZFC peak occurs at 30 K for the as-quenched sample. Upon annealing at temperatures below 500 °C, the peak temperatures

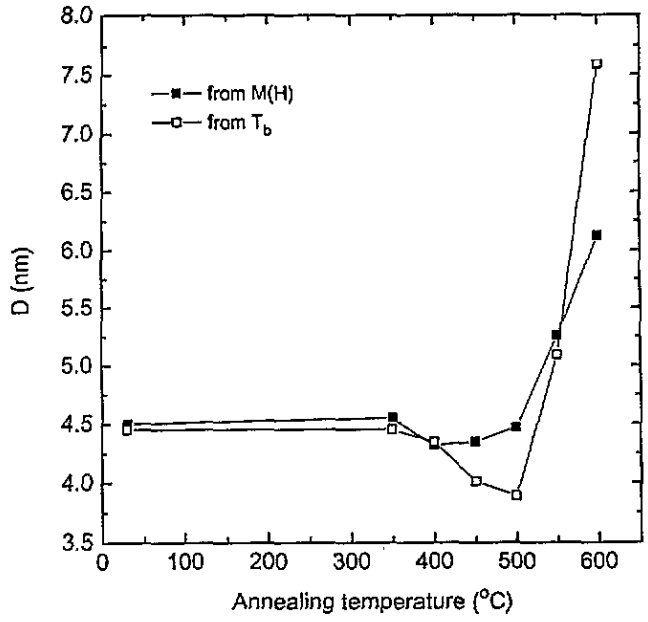

Figure 3. The Co particle diameter as a function of annealing temperature.

Table 1. Magnetic parameters determined from the magnetic measurement for $Co_{15}Cu_{85}$ samples annealed at various temperatures: M_s, saturation magnetization; M_r, magnetic remanence; H_c, coercivity; T_B, blocking temperature.

T (°C)	M_s (295 K) (emu g_{Co}^{-1})	M_r (295 K) (emu g_{Co}^{-1})	H_c (295 K) (Oe)	T_B (K)
Melt spun	87.20	15.33	164.0	30.0
350	81.90	14.75	170.0	30.0
400	91.14	15.58	175.0	45.0
450	99.42	10.08	184.0	22.0
500	131.43	26.75	185.0	20.0
550	147.38	40.92	213.0	60.0
600	146.28	45.83	252.0	149.0

in the ZFC data do not change very much. The sample annealed at $T = 600\,°C$ has a very broad peak near 150 K. In this annealing condition, some Co particles are still in the superparamagnetic regime, but some larger Co particles show re-entrant magnetic or ferromagnetic behaviour [23]. The higher freezing temperatures reflect the Co particle growth during annealing. As observed for sputtered samples [1, 8] and melt-spun Co–Cu alloys [30], a large thermal hysteresis is observed below a characteristic freezing temperature (above 320 K in figure 4), where the ZFC and FC curves diverge. The observation of thermal hysteresis much above the peak of the ZFC curves indicates the existence of a broad distribution in the sizes and shapes of the magnetic Co particles. As shown in figure 2 and figure 4(a), the as-quenched sample shows a large saturation magnetization and large thermal hysteresis between the ZFC and FC data. These results indicate that some Co clusters have already been formed during rapid solidification from the melt state. As reported in [23, 30], metastable Co_xCu_{1-x} alloys with $x \leqslant 0.20$ exhibit a rather

complex magnetic behaviour i.e. a mixture of paramagnetic and cluster-glass behaviours. The superparamagnetic contribution is associated with the very finely dispersed small Co clusters, and the cluster-glass contribution comes from the larger ferromagnetic Co clusters which are randomly distributed in the Cu matrix.

At a sufficiently high temperature (above the blocking temperature T_B), the magnetic anisotropy energy barriers of the single-domain particles are overcome by thermal fluctuation, and superparamagnetism occurs. Superparamagnetic behaviour can be observed using an instrument with a characteristic measuring time τ_i at the temperature above the blocking temperature T_B, which is defined as

$$T_B = \frac{E_a}{k_B \ln(\omega_0/\omega)} = \frac{K\langle V\rangle}{k_B \ln(\omega_0/\omega)} = \frac{K\langle V\rangle}{30k_B} \tag{3}$$

where $E_a = K\langle V\rangle$ is the magnetic anisotropy energy of the particles, K is the total magnetic anisotropy energy per unit volume and V is the volume of the magnetic particles. The factor of 30 represents $\ln(\omega_0/\omega)$, where ω is the inverse of the experimental time constant (about 1.0×10^{-2} Hz) and ω_0 is the attempt frequency (about 1.0×10^{11} Hz). Using the 0 K value of the magnetic anisotropy for FCC Co ($K = -2.7\times10^6$ erg cm^{-3}) [31,32], we have calculated the average Co particle size which agrees with that obtained from the magnetization fitting (figure 3).

The insets of figure 4 show the inverse susceptibility $1/\chi$ and its temperature dependence. The $1/\chi$ data are not linear in temperature T for the as-quenched samples or those annealed at temperatures below 500 °C. By considering interaction effects, following Chantrell and Wohlfarth [33], $\chi \propto M_s^2(T)/(T - T_0)$. $1/\chi$ is not linear in T because of the temperature dependence of $M_s(T)$. As the annealing temperature reached 600 °C, the growth of the Co particles results in an increase in the distance between the Co particles, and the magnetic Co particles are weakly interacting. In this case, the Co magnetic particles behave as non-interacting granules. This result was also verified by the good magnetization fitting using the Langevin equation using only single Co particles for the as-quenched sample annealed at a temperature of 600 °C (figure 2(a)). For a typical paramagnetic system with atomic moments, χ follows the well known Curie–Weiss law $\chi = np_{eff}^2\mu_B^2/3k_BT$. Thus, $1/\chi$ will be linear in T as shown in the inset of figure 4(d).

3.3. Giant magnetoresistance and relation to Co cluster size

Figure 5 shows the change in resistance with magnetic field for the samples in different states. The MR change was measured at 10 K and 295 K in maximum fields of 30 kOe and 50 kOe, respectively. The data are presented in the form of $\Delta R/R = [R(H) - R(H_{max})]/R(H_{max})$, where H_{max} is the maximum magnetic field. The field required to saturate the magnetoresistance is quite high for the sample in the as-quenched state and annealed at temperatures below 500 °C; $M(H)$ and MR are not saturated even in fields of 50 kOe. Here, we show only the GMR data in a maximum field of 30 kOe for comparison. We focus on the GMR at a low temperature (10 K), where the phonon and magnon contributions to the resistance are negligible.

In the as-quenched state the MR changes by as much as 16.0% in magnetic fields up to 30 kOe. Annealing of the as-quenched ribbons drastically increases the GMR as shown in figure 5. The maximum in the MR change of 43.0% was achieved for the sample annealed at 450 °C for 30 min, and a large slope $d(\Delta R)/dH$ was observed even in a field of 30 kOe. A high annealing temperature above 500 °C sharpens the $\Delta R(H)$ peaks at $H = H_c$ and increases the slope $d(\Delta R)/dH$ around $M = 0$. The apparent dependence of the GMR on

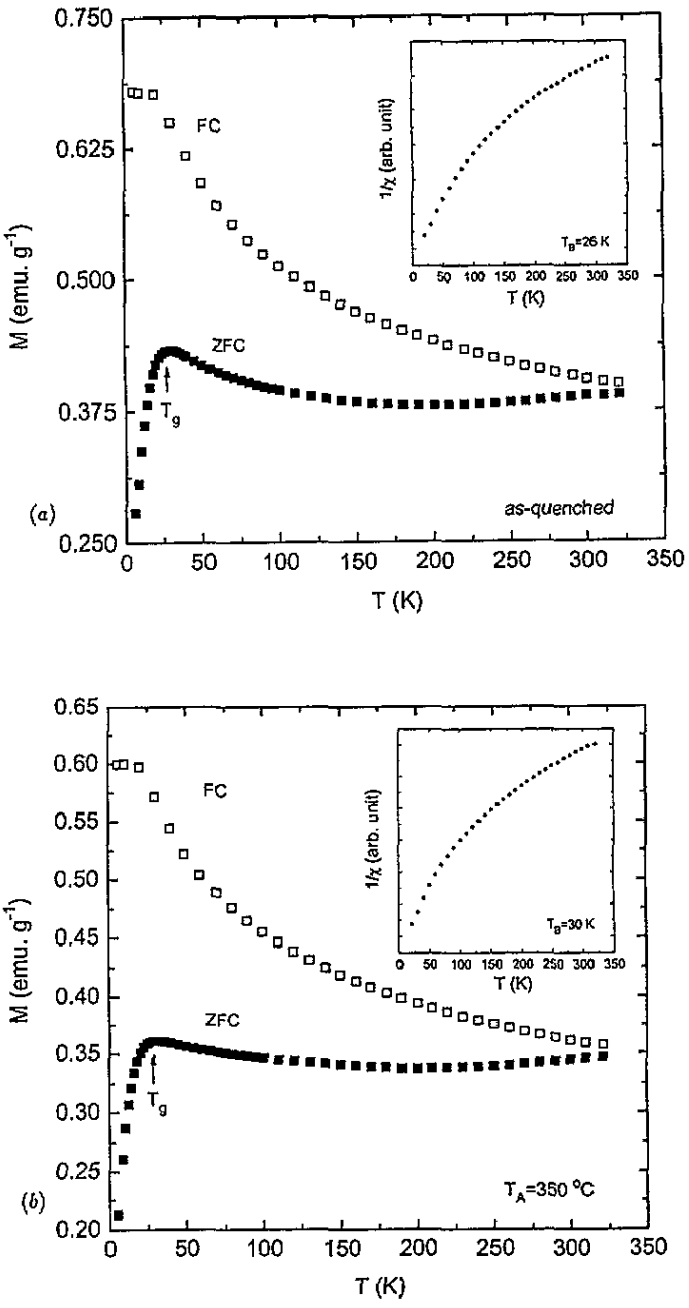

Figure 4. Magnetization of the $Co_{15}Cu_{85}$ samples in a field of 50 Oe both FC and ZFC: (a) as quenched; (b) annealed at 350 °C; (c) annealed at 500 °C; (d) annealed at 600 °C. The insets show the relation between the inverse susceptibility and temperature.

H is not revealed because the GMR is a direct consequence of the field dependence of the global magnetization [2]. The highest and lowest resistances were observed in the original unmagnetized state ($M = 0$) and in saturation state where all the particles were

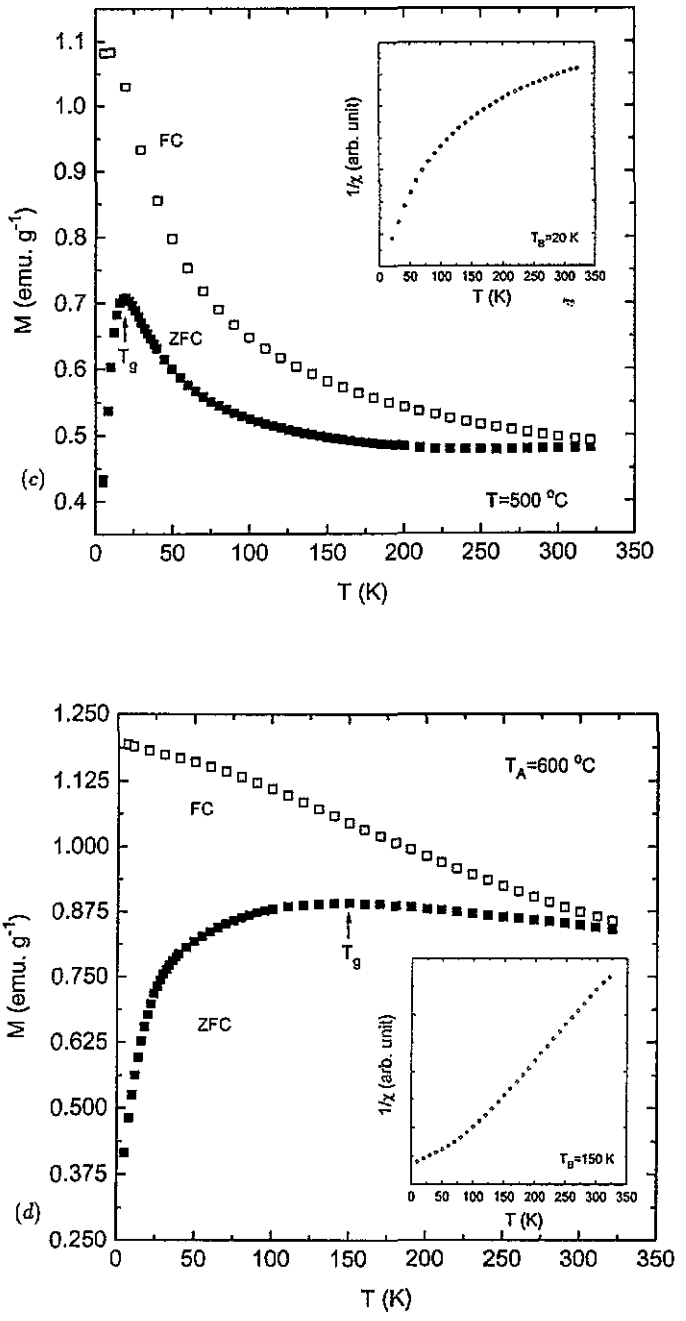

Figure 4. (Continued)

ferromagnetically aligned ($M = M_s$), respectively. The total resistivity change of the magnetic granular system is roughly expressed as [2] $\Delta R/R = -A_i(M/M_i)^2$, where A_i is the magnitude of the GMR which depends on the samples; this describes the GMR very well in a low magnetic field. In the granular systems, the important factor for the GMR is the average $\langle \cos\theta_{ij} \rangle$, where θ_{ij} is the relative angle between the axes of the ferromagnetic particles. If

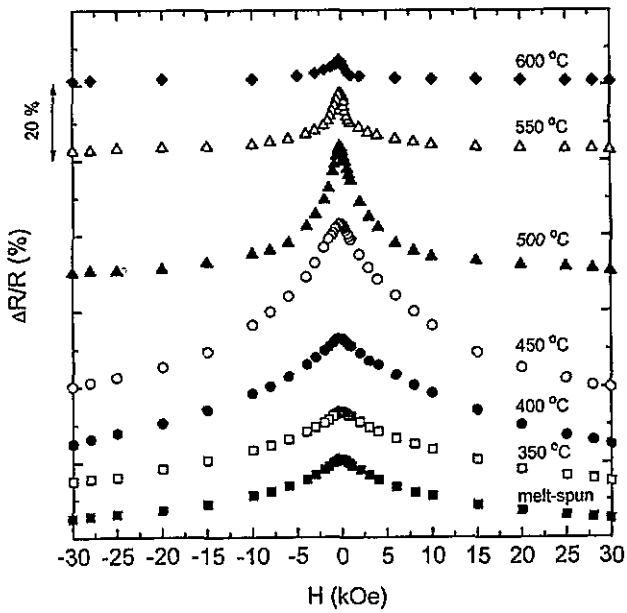

Figure 5. $\Delta R/R$ versus H for $Co_{15}Cu_{85}$ in the as-quenched and annealed states at 10 K.

all the magnetic particles are assumed to have the same magnetic moment $|m|$, then [27] $\langle \cos\theta_{ij} \rangle = \langle \cos\varphi_i \rangle^2 = M^2/M_s^2$, where φ_i is the angle between the magnetization axis of a particle and the external field, $\langle \cos\varphi_i \rangle$ is averaged over many ferromagnetic entities, and the relation between the GMR and global magnetization was roughly established. We found that this relation describes the experimental results in the magnetic fields of less than 2 kOe well, except for around $H = H_c$.

The dependence of the GMR on the annealing conditions is related to the change in the microstructure in the sample upon ageing, mainly the size of Co clusters and its distribution in the Cu matrix. The results in [2] show that there was a small change in MR (0.5%) in the homogeneous as-deposited samples of $Co_{20}Cu_{80}$ with magnetic fields of up to 50 kOe. At 10 K, however, we found that a MR change of as much as 16.0% was observed in the as-quenched ribbons. On the basis of the structural characterization using 295 K magnetization data, we assume that some magnetic domains with relatively low Co atom concentrations were formed during the rapid solidification, to which the MR change is attributed. Annealing the sample at a temperature below 500 °C, ultra-fine single-domain Co particles were nucleated in the Co-rich regions, and superparamagnetic behaviour appears. Annealing the as-quenched ribbon at 450 °C is appropriate for obtaining a higher GMR. At this temperature (450 °C), we can probably assume that the sample has higher magnetic particle surface-to-volume ratios which act as the conduction electron spin-dependent scattering centres. On further increase in the annealing temperature, the Co particles grow to a larger size; thus the GMR decreases owing to the reduction in the particle surface-to-volume ratios.

Figure 6 shows the relation between the MR and average Co particle size obtained from calculating the blocking temperature of Co magnetic particles. The fundamental assumption underlying models of GMR is that the current is carried in two independent conduction channels corresponding to spin-up and spin-down electrons. The field dependence of the resistivity is attributed to the spin-dependent scattering occurring within the magnetic

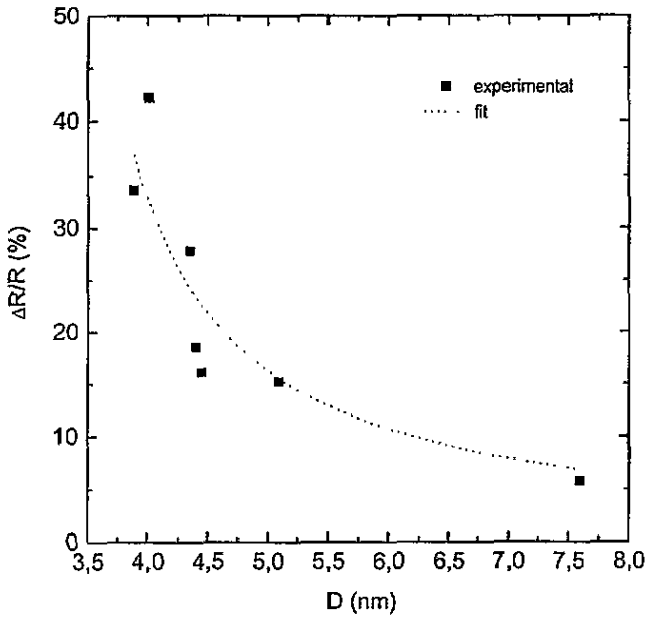

Figure 6. Dependence of $\Delta R/R$ on the average size of Co particles: ——, theoretical results.

clusters and at the magnetic and non-magnetic interfaces [5, 6]. As shown in figure 6, the MR increases with increasing ρ_{SV}, where ρ_{SV} is a measure of the surface-to-volume ratio of Co clusters and is proportional to $(4\pi r^2)/(4\pi r^3/3) = 3/r$, where r is the radius of Co particles. According to the phenomenological models described in [5, 6], the MR should scale approximately as the magnetic particle surface-to-volume ratio if interfacial spin-dependent scattering is the dominant mechanism for GMR in granular systems. Alternatively, if the spin-dependent volume scattering is dominant, then the MR should weakly depend on the magnetic particle size. We have examined the MR dependence upon Co cluster size by a representative model [5]

$$R(H) = \frac{\rho(H) - \rho(H_{max})}{\rho(H_{max})} = \frac{\rho_2^2}{\rho_1^2 - \rho_2^2}[1 - \alpha^2(H)] \tag{4}$$

where

$$\rho_1 = \frac{ck_F}{ne^2}\left(\frac{1 + p_b^2}{\lambda_m} + \frac{1 - c}{c\lambda_{nm}} + \frac{3(1 + p_s^2)}{r_m\lambda_s}\right) \tag{5a}$$

$$\rho_2 = \frac{ck_F}{ne^2}\left(\frac{2p_b}{\lambda_m} + \frac{6p_s}{r_m\lambda_s}\right) \tag{5b}$$

$$\alpha(H) = M(H)/M_s \tag{5c}$$

where c is the concentration of magnetic particles per unit volume, r_m is the average radius of the particles, p_b and p_s represent the ratios of spin-dependent to spin-independent scattering potentials in the magnetic particles and at the interfaces, λ_s is a parameter representing the interfacial roughness, and λ_m and λ_{nm} are the mean free paths for magnetic particles and the

non-magnetic matrix, respectively. Fitting the MR data to equation (4), we obtain $P_b = 0.18$, $P_s = 0.66$ and $\lambda_s = 3.5a_0$, and the fitting results are shown in figure 6. This analysis ($p_s > p_b$) provides quantitative confirmation that the interfacial spin-dependent scattering plays an important role underlying the GMR in the Co–Cu granular systems. According to equation (3), the key parameters are the mean free path, the ratio of spin-dependent to spin-independent scattering potentials, and the interfacial roughness. For the small magnetic particles, they will be subject to thermally activated magnetization which adversely affects the MR change [1]. The magnetic particle size dependence of GMR should exhibit a peak behaviour.

4. Conclusions

We have investigated the microstructure, magnetic properties and GMR of $Co_{15}Cu_{85}$ samples in the as-quenched state and annealed at different temperatures. The materials consist of nanometre-sized Co magnetic particles embedded in a Cu non-magnetic matrix. The MR change with magnetic field is closely correlated with the Co particle size and density. The average Co particle diameter ranges from 3.5 to 8.0 nm for the sample annealed at temperatures below 600 °C, which results in a change in the magnetic properties and a change in the value of the GMR. The GMR decreases with increasing Co particle size. The largest GMR occurs for the sample annealed at 450 °C for 30 min, which results in an average Co particle size of 4.0 nm. In our experiment, a universal variation in GMR with particle size has been revealed. The phase separation is crucial for the GMR in magnetic granular systems.

References

[1] Berkowitz A E, Mitchell J R, Carey M J, Young A P, Zhang S, Spada F E, Parker F T, Hutten A and Thomas G 1992 *Phys. Rev. Lett.* **68** 3745
[2] Xiao J Q, Jiang J S and Chien C L 1992 *Phys. Rev. Lett.* **68** 3749
[3] Camley R E and Barnas J 1989 *Phys. Rev. Lett.* **63** 664
[4] Levy P M, Zhang S and Fert A 1990 *Phys. Rev. Lett.* **65** 1643
[5] Zhang S and Levy P M 1993 *J. Appl. Phys.* **73** 5315
[6] Zhang S 1992 *Appl. Phys. Lett.* **61** 1855
[7] Barnard J A, Waknis A, Tan M, Haftek E, Parker M R and Watson M L 1992 *J. Magn. Magn. Mater.* **114** L230
[8] Carey M J, Young A P, Starr A, Rao D and Berkorwitz 1992 *Appl. Phys. Lett.* **61** 2935
[9] Tsoukatos A, Wan A H, Hadjipanayis G C and Unruth K M 1993 *J. Appl. Phys.* **73** 5509
[10] Watson M L, Barnard J A, Hossain S and Parker M R 1993 *J. Appl. Phys.* **73** 5506
[11] Kneller E 1963 *J. Appl. Phys.* **33** 1355
[12] Chien C L, Liou S H, Xiao G and Gatzke M A 1993 *Science and Technology of Rapidly Quenched Alloys (Mater. Res. Soc. Symp. 80)* (Pittsburgh, PA: Materials Research Society) p 395
[13] Cabañas-Moreno J G, Lopez V M, Calderon H A and Redon-Angeles J C 1993 *Scr. Metall.* **28** 645
[14] Gente C, Oehring O and Burmann R 1993 *Phys. Rev. B* **48** 13244
[15] Wecker J, von Helmolt R, Schultz L and Samwer K 1993 *Appl. Phys. Lett.* **62** 1985
[16] Dieny B, Chamberod A, Genin J B, Rodmacq B, Teixeira S R, Auffret S, Gerald P, Redon O, Pierre J, Ferrer R and Barbara B 1993 *J. Magn. Magn. Mater.* **126** 433
[17] Takeda H, Kataoka N, Fukamichi and Shimada Y 1994 *Japan. J. Appl. Phys.* **33** L102
[18] Ghannami M E, Polo C G, Rivero G and Hernando A 1994 *Europhys. Lett.* **26** 701
[19] Yu R H, Zhu J, Zhang X X and Knbel M 1995 *J. Mater. Sci. Technol.* submitted
[20] Nishizawa T and Ishida K 1984 *Bull. Alloy Phase Diagram* **5** 161
[21] Le Goues F K and Aaronson H I 1984 *Acta Metall.* **32** 1855

[22] Wagner W 1989 Z. *Metallkd.* **80** 873
[23] Childress J R and Chien C L 1991 *Phys. Rev.* B **43** 8089
[24] Grangle J 1955 *Phil. Mag.* **46** 499
[25] Childress J R and Chien C L 1991 *J. Appl. Phys.* **70** 5885
[26] Bean C P and Livingston J D 1959 *J. Appl. Phys.* **32** 120S
[27] Khanna S N and Linderoth S 1991 *Phys. Rev. Lett.* **67** 742
[28] Grangvist C G and Burman R A 1976 *Solid State Commun.* **18** 123
[29] Grangvist C G and Burman R A 1976 *J. Appl. Phys.* **47** 2200
[30] Dieny B, Chamberod A, Cowache C, Genin J B, Teixeira S R, Ferre R and Barbara B 1994 *J. Magn. Magn. Mater.* **135** 191
[31] Sucksmith W A and Thompson J E 1954 *Proc. R. Soc. (London)* A **225** 362
[32] Doyle W D and Flanders P J 1964 *Proc. Int. Conf. on Magnetism (Nottingham, 1964)* p 751
[33] Chantrell R W and Wohlforth E P 1983 *J. Magn. Magn. Mater.* **40** 1